

Global Air Pollution Potential: long term (1980-2019) trends and application to sustainable development

Hareef baba shaeb Kannemadugu (✉ babaphyway@gmail.com)

National Remote Sensing Centre, ISRO (Department of Space–Government of India)

Sandelger Dorligjav

National University of Mongolia

Alok Taori

National Remote Sensing Centre, ISRO (Department of Space–Government of India)

Rajashree Vinod Bothale

National Remote Sensing Centre, ISRO (Department of Space–Government of India)

Prakash Chauhan

National Remote Sensing Centre, ISRO (Department of Space–Government of India)

Article

Keywords: Air pollution potential, Ventilation coefficient, Sustainable development, PM2.5, AOT

Posted Date: August 24th, 2023

DOI: <https://doi.org/10.21203/rs.3.rs-2888054/v1>

License:  This work is licensed under a Creative Commons Attribution 4.0 International License.

[Read Full License](#)

Additional Declarations: No competing interests reported.

Abstract

Air pollution potential is a measure of the inability of the atmosphere to disperse pollutants away from the source. It depends on Planetary Boundary Layer Height (PBLH) and wind speed. Global air pollution potential Index (APPI) maps have been generated for the first time using 40 years (1980–2019) of PBLH and wind speed data available from ERA5 reanalysis data. These are useful for identifying ventilation corridors and for sustainable development. The seasonal climatology of APPI is also analyzed. Long-term trends in Ventilation coefficient (VC), PBLH, Wind speed, PM_{2.5}, and Aerosol Optical Thickness (AOT) were analyzed globally and in over 30 cities to understand their future impact on climate change scenarios. High APPI is observed in the south Asian Regions, giving rise to PM_{2.5} and AOT hot spots, and are naturally disadvantageous. Long-term trends in VC and associated trends in PBLH and Wind speed suggest that the PBLH is decreasing at the rate of 1–3 m per year over south Asia, and wind speed is decreasing at the rate of 0.01–0.02 m·s⁻¹ per year, resulting in the decrease of VC of about 1–25 m²·s⁻¹ per year. If this trend continues, South Asia will have more air pollution potential in the coming years putting health risks to 1.8 billion people. The surface PM_{2.5} and AOT is increasing at 0.5–1.5 µg·m⁻³ per year and 0.005–0.01 per year for south Asia cities. Sustainable development goals and climate policies/negotiations should consider global air pollution potential as an essential variable in planning and mitigation.

Introduction

Air pollution has recently been the primary concern as it affects human health and is accountable for about 90 lakh deaths per annum^{1,2}. The World Health Organization (WHO) reported that 92% of the global population inhales unclean air with annual mean PM_{2.5} exceeding 10 µg·m⁻³ leading to diseases related to the lungs and heart^{3,4}. Cities are more fuller vulnerable to air pollution due to vehicular and industrial emissions, and the Sustainable Development Goal (SDG) target 11.6 calls for reducing adverse environmental effects in cities^{3,5}. Most south Asian cities are at risk due to high population density and require quick policy responses⁶. UN Environment Programme and WMO linked pollution reduction to climate change mitigation⁷. The 2017 Lancet commission documented that pollution control can mitigate the effects of other threats, such as climate change and biodiversity loss¹. Therefore, identifying ventilation corridors or sites with low air pollution potential will aid in sustainable development, reducing the effects on humans⁸.

The Planetary Boundary-Layer Height (PBLH) is a crucial parameter that affects the vertical extent of the mixing of air pollutants and, thus, dispersion⁹. PBLH is estimated using in situ measurements such as Radiosonde, LIDAR^{10,11} or satellite-based methods such as Radio Occultation (GPSRO) and Atmospheric sounders (AIRS, CrIs, etc.)¹². However, these methods are limited by spatial and temporal coverage. Reanalysis data sets such as ERA5 and MERRA-2 overcome this limitation and have proven to be most

promising for different applications^{13,14}. Another variable influencing air pollution dispersion is the average wind speed within the boundary layer, provided by ERA5¹⁵

The Ventilation coefficient (VC) is a product of PBLH and the average wind speed within the PBLH¹⁶. VC is a good indicator of air pollution potential, i.e., a measure of the inability of the atmosphere to disperse the pollutants away from the source¹⁷⁻¹⁹. Some authors use assimilative capacity, which is the ability of the atmosphere to dilute pollutants²⁰. Using Air Pollution Potential Index (APPI), the regions with low air pollution potential can be demarcated as ventilation corridors and are essential in understanding the impact on air quality caused by the future establishment of Industries. APPI is also helpful for prioritizing the areas for mitigation measures by the policymakers. The health department can also use this information on air pollution potential to advise tourists with respiratory and heart diseases on the potential threat to their health. This index is also helpful for several other people, such as agriculturalists (forest officials), to study possible effects on crop growth (forest growth) in regions with high APPI; Ornithologists to study effects on birds' population and migration due to unfavorable conditions. The real estate sector or planning departments also find this helpful to build sustainable building infrastructure. It is also possible that policymakers can decide where the budget needs to be invested more in health insurance premiums for the public or provide health centers.

Few researchers studied air pollution potential derived from ventilation coefficient in different countries in the World, such as the USA^{16,17,21,22}, India^{18,23,24}, Argentina²⁵, Nigeria²⁶, and Mongolia²⁷. These studies mostly used Radiosonde data to derive the ventilation coefficient and are limited by spatial extent. Recently, Hareef baba shaeb et al.⁸ used a satellite sensor (SNPP-CrIs) derived PBLH and ERA5 wind speed to derive ventilation coefficient and spatial maps of air pollution potential over India.

The current study utilizes 40 years (1980-2019) of PBLH and wind speed data from ERA5 reanalysis data to generate global air pollution potential maps. We also looked at long-term trends in APPI, VC, PBLH, Wind speed, PM2.5, and Aerosol Optical Thickness (AOT) to understand their future impact in climate change scenarios. The objectives are as below:

1. To prepare 40-year mean annual and seasonal Global air pollution potential maps and analyze its spatial variation.
2. To analyze long-term global trends in APPI, PBLH, Wind speed, PM2.5, and AOT
3. To analyze long-term trends in APPI, PBLH, Wind speed, PM2.5, and AOT in capital cities of 30 countries

As the world population is going to touch 8.5 billion by 2030, air pollution poses a significant risk to health and climate due to increased anthropogenic activities such as vehicular pollution and Industrial emissions. These Global APPI maps can be used for planning and mitigation measures and aid sustainable development. Air pollution is a global problem, and associated health response varies from country to country²⁸. Therefore, the air pollution potential maps are prepared at a global level. Along with the rapid development and population growth of countries around the world, urbanization and

industrialization are intensifying the conditions of air pollution^{29,30}. In other words, the level of air pollution in countries depends on their development, population density, and geographical conditions^{31,32}. Therefore, the study area is selected based on the characteristics mentioned above. Fig.1a and Fig.1b represent the spatial distribution of the capital cities of the 30 largest countries as an area in the world³³ with the ESRI land cover map in the background and population density, respectively. Fig.1b shows that countries in south Asia possess very high population densities compared to the rest of the world and are at higher risk of air pollution.

Results

Spatial variation in Global air pollution potential

Figure 2a shows the spatial variation of the annual mean ventilation coefficient / APPI obtained using the monthly data from 40 years (1980–2019). U.S. National Weather Service³⁴ and Atmospheric Environment Service Canada uses VC criteria of high ($< 6000 \text{ m}^2 \cdot \text{s}^{-1}$), medium ($6000\text{--}12,000 \text{ m}^2 \cdot \text{s}^{-1}$), and low pollution potential ($> 12,000 \text{ m}^2 \cdot \text{s}^{-1}$). However, based on the variability of VC over the Globe, the Ventilation coefficient has been categorized into six different pollution potential zones or APPI, as shown in Table 1. Hareef baba shaeb et al.⁸ has used similar criteria.

Table.1. List of Air Pollution Potential Index (APPI) categories

VC ($\text{m}^2 \cdot \text{s}^{-1}$)	APPI	Pollution potential category
0–1000	1	Very High
1000–2000	2	High
2000–4000	3	Medium
4000–8000	4	Below medium
8000–10,000	5	Low
> 10,000	6	Very low

Below medium to very low air pollution potential Index is observed in Argentina, Eastern Brazil, Ethiopia, Somalia, the northern territory of Australia, the Tibetan plateau, parts of Egypt, Niger, Western Sahara, and the northernmost of the Antarctic coast. These regions or ventilation corridors are most suitable for establishing future industries and have critical applications for the health sector, Agriculture/forestry, and Tourism sector. Global organizations such as the United Nations can take up sustainable developmental projects in these regions.

Medium Air pollution potential Index is observed in parts of South America (northern parts of Venezuela and Guyana, North-eastern Brazil, parts of west Argentina and Bolivia), North America (Northern Mexico,

southern US, Eastern Canada), Africa (northern Africa, Zambia, Zimbabwe, Botswana, southern part of South Africa), Northern Madagascar, Arabian peninsula except Jordan and Oman, parts of Iran, western Pakistan, Afghanistan, Kyrgyzstan, western India (excluding the western Ghats), Europe (Ireland, UK, Germany, Poland, Denmark, Belarus), Russia (some central parts), Northeast China, Northern Japan and most of Australia (except the southeast, southwest and southernmost central regions). These regions can be considered as medium ventilation corridors and rank next to the ventilation corridors suitable for sustainable development. Compared to below medium to very low potential regions, these regions occupy more spatial extent. Hence, policymakers can use these areas to develop tourism, Industries, Agriculture/forestry, and the health sector (rehabilitation homes for those vulnerable / high risks to high concentrations of air pollution).

A high to very high air pollution potential Index is observed in the rest of the regions in the globe. Especially very high APPI regions need to be notified and monitored. The people living in these areas will be most vulnerable to the health effects of air pollution and associated mortality. The authorities can issue a health advisory to people with existing heart and lung diseases coming into this area who should take proper precautions to avoid heart or Asthma attacks. These areas also carry associated soil pollution due to rain washing out the aerosols and later missing with the soil. Policymakers also can see that their developmental plans reduce the population density in these areas to reduce the risk to the large population. Most importantly, regions covering Alaska, Greenland, Iceland, and most parts of Antarctica fall into this category. This means climate change effects induced by stagnated pollutants transported from elsewhere into these regions or locally produced by the ship emissions will be significant.

Figure 2b and Fig. 2c show the spatial variation of PBLH and mean wind speed obtained using the monthly data from 40 years (1980–2019). The boundary layer height is one of the critical meteorological parameters confining the vertical mixing of air pollutants. High PBLH areas coincide with the high VC areas (in Fig. 2), indicating that the ventilation is due to vertical mixing. In some regions though vertical mixing is moderate (PBLH- 425–580 m), the VC is low as there are low wind speeds ($0-2 \text{ m}\cdot\text{s}^{-1}$), e.g., in the Indo-Gangetic plain (IGP). High Wind speed regions shown in Fig. 2c help develop alternate wind energy solutions for sustainable development, avoiding the air polluting industries.

Figure 3a and Fig. 3b show the spatial variation of surface PM_{2.5} concentration and AOT obtained using the monthly data from 40 years (1980–2019). It can be observed that most of the globe exceeded the WHO clean air limit of PM_{2.5} above $10 \mu\text{g}\cdot\text{m}^{-3}$, and the average PM_{2.5} exceeded three times the limit in the medium to very high pollution potential regions (Fig. 2). The vehicular /Industrial emissions probably cause this due to high population density in the south Asia and sand and dust storms in the North Africa and Arabian Peninsula³⁵.

From Fig. 3b, it can be seen that aerosol optical thickness (total aerosol burden in the atmospheric column) is lower in the regions of very low air pollution potential (ventilation corridors); alternatively, AOT values are higher in the regions where APPI is high. This correlation also depends on the population density (Fig. 1b) in that particular region and the presence of anthropogenic /natural pollution sources.

Hence, those regions with naturally poor ventilation corridors (Very high APPI) tend to give hotspots in the air pollution detected by the satellites. Whereas in those regions classified as ventilation corridors (low APPI), the emissions may be higher but will not lead to hot spots. In effect, the regions with high pollution potential are naturally disadvantageous, and climate policies/negotiations should not penalize these regions. Moreover, climate negotiations should aim to aid these regions in developing cleaner technologies.

Seasonal climatology of APPI:

Figure 4 shows that the APPI varies seasonally over the Globe, with significant spatial changes observed during MAM and JJA compared to DJF and SON. These changes can be attributed to the high temperature and circulation changes, which increase the PBLH and wind speed, respectively, during the spring (MAM) and Summer (JJA) seasons, especially in the tropics and subtropics. These changes can be noticed especially in Arabian Peninsula and South Asian region. These regions have medium to low air pollution potential during MAM and JJA compared to DJF and SON. This information is helpful for the health advisory for people suffering from lung and cardiovascular diseases. The policymakers can also insist on maximum production from air-polluting industries during these seasons to reduce the effects on human health. These seasonal global air pollution potential maps help plan to mitigate the effects of air pollution and site selection to establish new industries.

Long term trends in VC, PBLH and wind speed and associated air quality changes (PM_{2.5} and AOT)

It is essential to understand the long-term trends in VC and associated trends in PBLH and Wind speed to understand the air pollution potential changes at the global level and identify more vulnerable regions. Figure 5b shows that the PBLH is decreasing at the rate of 1–3 m over south Asia, and Fig. 5c shows that the wind speed is decreasing at the rate of 0.01–0.02 ms⁻¹ resulting in a decrease of VC of about 1–25 m²·s⁻¹ (Fig. 5a), respectively. This means South Asia will have more air pollution potential in the coming years, which means people living in these areas are more vulnerable to diseases caused by air pollution. Urgent mitigation and control measures are needed to tackle the increasing air pollution. Apart from emissions caused by anthropogenic factors, decreasing VC, i.e., increasing air pollution potential responsible for making this region a hot spot for air pollution over the globe.

PM_{2.5} is the most dangerous to human health compared to other criteria air pollutants. The most common anthropogenic sources are fossil fuel-based vehicular pollution, Industries, agriculture waste, and biomass burning. Due to their small size (2.5 microns) can penetrate the inner parts of the lungs upon inhalation and cause asthma, lung cancer, and heart diseases³⁶. Ellis and Roberts⁶ reported that annual mean PM_{2.5} concentrations and population density for south Asia cities are strongly correlated, and a doubling of population density is associated with a 34.8% increase in PM_{2.5}. In contrast, in other cities, it is 24.2%. This anomaly may be due to the decreasing trend in VC in south Asia, which tends to assimilate pollution instead of dispersing away, leading to increased local surface concentrations. Figure 6a and Fig. 6b show that surface PM_{2.5} concentration and AOT are increasing at a rate of 0.5–1.5

$\mu\text{g}\cdot\text{m}^{-3}$ and 0.005-0.1, respectively. The Global trends in PM2.5 and AOT observed match well with that reported by Hammer, et al. ³⁷.

A decreasing trend in the BLH is observed in several other parts of the globe, namely western Australia, parts of Africa, and South America. Figure 5c shows a decreasing trend in the windspeed in several parts of the globe. These trends in BLH and Wind speed resulted in the different spatial distributions in long-term trends in VC (Fig. 5a). The VC is decreasing ($1-25 \text{ m}^2\cdot\text{s}^{-1}$ per year) in south asia, Europe, west Africa, Northern parts of south America, East Canada while it shows an increasing ($1-35 \text{ m}^2\cdot\text{s}^{-1}$ per year) trend in Australia, the Tibetan plateau, the central part of Russia, major parts of western Asia, Arabian peninsula, Eastern parts of Africa, South America, the USA, and west Canada. Figure 5a, and Fig. 6 show that the regions (except Europe) showing the decreasing trend in the VC show an increasing trend in the PM2.5 concentration and columnar loading of the aerosols. This correlation has important implications for planning mitigation measures and sustainable development. The climate negotiations also should focus on creating clean energy and fuel-efficient solutions in this area with funding from United Nations or developed countries.

Trends in VC, BLH, Wind speed and associated air pollution (PM2.5, AOT) over world cities

Cities with high population density are at the forefront of air pollution impact by increasing vehicular and industrial emissions³. Hence, It is essential to understand the trends of VC (air pollution potential) and air pollution (PM2.5 and AOT) over the world cities to control urban air pollution and decrease the harmful effects on people's health.

Figure 7 shows annual trends in VC/Air pollution potential, PM2.5, and AOT over global cities. Figure 7a shows that VC is decreasing (APPI is increasing) at the rate of 5 to 12 $\text{m}^2\cdot\text{s}^{-1}$ per year in Mexico, Ottawa, Niamey, Luanda, and New Delhi. This decreasing VC is very alarming for these cities; due to the high air pollution potential index, the pollutants will stagnate and pose a severe threat to people in these cities. At Khartoum and Riyadh, VC is increasing at the rate of 8.7–15 $\text{m}^2\cdot\text{s}^{-1}$ while increasing at the lesser rate of 0- 8.7 $\text{m}^2\cdot\text{s}^{-1}$ at Brasilia, Addis Ababa, Tehran, Ulaanbaatar, and Jakarta. In the rest of the cities under study, the trend in VC is non-significant.

Figure 7b shows that PM2.5 concentration is increasing at the rate of 0 to 1.23 $\mu\text{g}\cdot\text{m}^{-3}$ per year in Mexico, Bogota, Lima, La Paz, Luanda, Pretoria, Cairo, Khartoum, Addis Ababa, Riyadh, Tehran, New Delhi, Beijing, and Jakarta. PM2.5 concentration is decreasing at the rate of 0 to 0.36 $\mu\text{g}\cdot\text{m}^{-3}$ per year in Washington DC, Ottawa, Nouakchott, and Moscow. In the rest of the cities under study, the trend in PM 2.5 is non-significant.

Figure 7c shows that AOT is increasing at 0 to 0.009 per year at Bogota, Lima, Cairo, Addis Ababa, Riyadh, New Delhi, Beijing, and Jakarta. AOT is decreasing from 0 to 0.005 at Pretoria, Mexico, Washington DC, Ottawa, Nuuk, Algiers, Tripoli, Bamako, Niamey, N Djamena, Kinshasa, Moscow, Astana, and Ulaanbaatar. In the other cities under study, the trend in AOT is non-significant.

Discussion

Global air pollution potential maps have been generated for the first time using 40 years (1980–2019) of PBLH and wind speed data available from ERA5 reanalysis data. The seasonal climatology of VC is also analyzed. Long-term trends in VC, PBLH, Wind speed, PM_{2.5}, and AOT were analyzed globally and in over 30 cities to understand their future impact in climate change scenarios. Argentina, Eastern Brazil, Ethiopia, Somalia, the northern territory of Australia, the Tibetan plateau, parts of Egypt, Niger, Western Sahara, and the northernmost part of the Antarctic coast have below medium to very low air pollution potential Index. These regions are ventilation corridors and are most suitable for sustainable development without causing much harm to human health. The Medium Air pollution potential Index is observed in several parts of the globe and occupies more spatial extent than below medium to very low potential regions. A high to very high air pollution potential Index is observed in the rest of the regions (most importantly Alaska, Greenland, Iceland, and most of Antarctica). These areas will be most vulnerable to climate change, air pollution's health effects, and associated mortality. Regions such as South Asia, which gives rise to hot spots in AOT and PM_{2.5}, have high air pollution potential Index (1–2), are naturally disadvantageous, and climate policies/negotiations should not penalize these regions. Moreover, climate negotiations should aim to aid these regions in developing cleaner technologies. Long-term trends in VC and associated trends in PBLH and Wind speed suggest that the PBLH is decreasing at the rate of 1–3 m over south Asia, and wind speed is decreasing at the rate of 0.01–0.02 m·s⁻¹ resulting in a decrease of VC of about 1–25 m²·s⁻¹ respectively. This VC decrease means south Asia will have more air pollution potential in the coming years, which means people living in these areas are more vulnerable to diseases caused by air pollution. Urgent mitigation and control measures are needed to tackle the increasing air pollution. Apart from emissions caused by anthropogenic factors decreasing VC, i.e., increasing air pollution potential is making these regions hot spots of air pollution globally. For south Asia cities, the surface PM_{2.5} and AOT are rising at a rate of 0.5–1.5 µg·m³ and 0.005–0.1, respectively. A decreasing trend in the VC is observed (1–25 m²·s⁻¹ per year) in south Asia, Europe, west Africa, Northern part of south America, East Canada while it shows an increasing (1–35 m²·s⁻¹ per year) trend in Australia, the Tibetan plateau, the central part of Russia, major parts of western Asia, Arabian peninsula, Eastern parts of Africa, South America, the USA, and west Canada. The regions (except Europe) showing the decreasing trend in the VC show an increasing trend in the PM_{2.5} concentration and columnar aerosol loading. This has important implications for planning mitigation measures and sustainable development. VC is decreasing (APPI is increasing) at 5 to 12 m²·s⁻¹ per year in Mexico, Ottawa, Niamey, Luanda, and New Delhi. This decreasing VC is alarming for these cities; due to the high air pollution potential index, the pollutants will stagnate and severely threaten people in these cities. At Khartoum and Riyadh, VC is increasing at 8.7–15 m²·s⁻¹ per year while increasing at the lesser rate of 0–8.7 m²·s⁻¹ at Brasilia, Addis

Ababa, Tehran, Ulaanbaatar, and Jakarta. PM_{2.5} concentration is increasing at 0 to 1.23 µg·m⁻³ per year in Mexico, Bogota, Lima, La Paz, Luanda, Pretoria, Cairo, Khartoum, Addis Ababa, Riyadh, Tehran, New Delhi, Beijing, and Jakarta. PM_{2.5} concentration decreases at 0 to 0.36 µg·m⁻³ per year in Washington DC, Ottawa, Nouakchott, and Moscow. AOT is increasing at 0 to 0.009 per year at Bogota, Lima, Cairo, Addis Ababa, Riyadh, New Delhi, Beijing, and Jakarta. AOT is decreasing from 0 to 0.005 at Pretoria, Mexico, Washington DC, Ottawa, Nuuk, Algiers, Tripoli, Bamako, Niamey, N Djamena, Kinshasa, Moscow, Astana, and Ulaanbaatar.

Methods

Determination of average wind speed within the PBL and VC calculation from ERA5 reanalysis data

The fifth generation of the European Centre for Medium-Range Weather Forecasts (ERA5) provides global high-resolution atmospheric reanalysis data at the single and pressure levels. The Climate Data Store (<https://cds.climate.copernicus.eu/cdsapp#!/home>) contains the hourly and monthly ERA5 data with a horizontal grid of 0.25°×0.25° from 1959 to the present¹⁵. The present study used the monthly PBL height (PBLH), orography, surface pressure, and temperature at a single level, as well as zonal and meridional wind components at pressure levels for a global scale from 1980 to 2019. von Engel and Teixeira³⁸ reported an excellent agreement of PBLH derived from radiosonde and ERA5 data for both mean and standard deviation. The bulk Richardson number method measuring the atmospheric conditions is used in the PBLH calculation^{15,39}. Moreover, Ramon, et al.⁴⁰ suggested that ERA5 mean wind speeds showed the best estimate compared to other reanalysis products.

The pressure at the top of PBLH was estimated from the single-level data using the hypsometric equation (Eq. 1).

$$p_{PBLH} = p_s e^{-\frac{g(PBLH+h_s)}{R_d T}}$$

1

Where: PBLH- PBLH above ground level (m), h_s - surface elevation above the mean sea level (m), p_s -the surface pressure (hPa), p_{PBLH} - pressure at the top of PBLH (hPa), R_d - gas constant for dry air, g - gravitational acceleration, T – absolute air temperature (K).

Wind speeds below the derived pressure level were globally averaged at every grid of 0.25° for a given time from the pressure levels data from 1980 to 2019. The estimated average wind speeds are vital variables for deriving the atmospheric ventilation coefficient (VC)^{41,42}.

The multiplication of PBLH and mean wind speed within the PBL^{8,42} at each grid point of global data for a given time gives the VC (Eq. 2).

$$VC = PBLH \bullet V$$

2

Where: \bar{V} - mean wind speed within the PBL ($m \cdot s^{-1}$), VC - atmospheric ventilation coefficient ($m^2 \cdot s^{-1}$).

Spatiotemporal trend analysis of GAPP/VC, PBLH, average wind speed, PM2.5 and, AOT

The main calculations of this study were to derive monthly average wind speed within PBL and VC from ERA5 data using Eqs. (1) and (2), respectively, from 1979 to 2019. Later long-term seasonal and annual average maps for PBLH, wind speed, and VC were plotted and analyzed globally using Arc GIS software. Seasons considered are winter (DJF, December-January-February), spring (MAM, March-April-May), summer (JJA, June-July-August), and autumn (SON, September-October-November).

The Modern-Era Retrospective Analysis for Research and Application, version 2 (MERRA-2), apart from meteorological reanalysis, also includes the assimilation of aerosol observations based on the GEOS-5 model coupled to the Goddard chemistry, aerosol, radiation, and transport (GOCART) aerosol module. It contains the assimilation of AOT from MODIS sensors, the AVHRR instruments, MISR, and AOT from the AERONET^{43,44}. The aerosol components were obtained from M2TMNXAER two-dimensional, monthly time-averaged aerosol diagnostics files (tavgM_2d_aer_Nx)⁴⁵ at a spatial resolution of $0.5^\circ \times 0.625^\circ$.

The Spatial trend analysis of PBLH, Wind speed, VC, PM 2.5 and AOT over the globe has been done using the annual averages of these parameters. The trend analysis for these parameters is done for capital cities of the largest 30 countries (Fig. 1).

Declarations

Competing interest

The Authors declare no Competing Financial or Non-Financial Interests

Data Availability

ERA-5 data are obtained from

<https://www.ecmwf.int/en/forecasts/dataset/ecmwf-reanalysis-v5>

MERRA-2 data are obtained from

<https://gmao.gsfc.nasa.gov/reanalysis/MERRA-2>

Author Contributions

H.B.S.K and S.D. conceived the study, performed the analyses, and wrote the manuscript. A.T., R.V.B, and P.C. contributed to revising the paper and assisted in interpretation of the results.

References

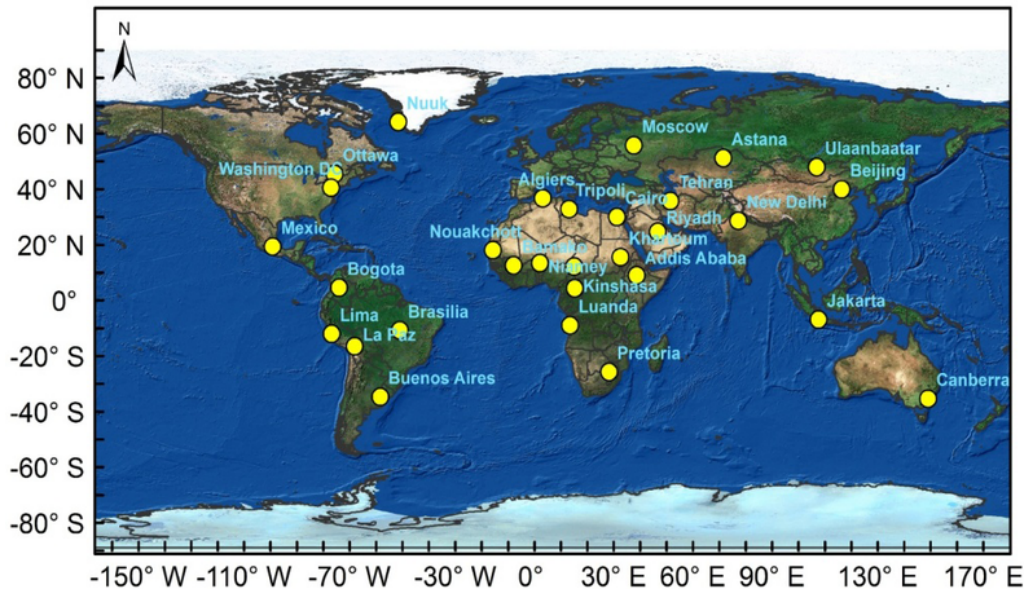
1. Fuller, R. *et al.* Pollution and health: a progress update. *The Lancet Planetary Health***6**, e535-e547 (2022). [https://doi.org/10.1016/S2542-5196\(22\)00090-0](https://doi.org/10.1016/S2542-5196(22)00090-0)
2. Cao, Z., Zhou, J., Li, M., Huang, J. & Dou, D. Urbanites' mental health undermined by air pollution. *Nature Sustainability* (2023). <https://doi.org/10.1038/s41893-022-01032-1>
3. HEI, Health Effects Institute. 2019. State of Global Air 2019. Special Report. Boston, MA: Health Effects Institute
4. Gakidou, E. *et al.* Global, regional, and national comparative risk assessment of 84 behavioural, environmental and occupational, and metabolic risks or clusters of risks, 1990–2016: a systematic analysis for the Global Burden of Disease Study 2016. *The Lancet***390**, 1345-1422 (2017). [https://doi.org/https://doi.org/10.1016/S0140-6736\(17\)32366-8](https://doi.org/https://doi.org/10.1016/S0140-6736(17)32366-8)
5. Alvarez, G. R., Lambrechts, M. & Wadhwa, D. "Polluted air plagues cities worldwide" In Atlas of the Sustainable Development Goals 2020: From World Development Indicators, edited by A. F. Pirlea, U. Serajuddin, D. Wadhwa, M. Welch and A. Whitby. (World Bank. <https://datatopics.worldbank.org/sdgoalatlas/goal-11-sustainable-cities-and-communities/>. License: Creative Commons Attribution CC BY 3.0 IGO, Washington, DC, 2020).
6. Ellis, P. & Roberts, M. *Leveraging Urbanization in South Asia: Managing Spatial Transformation for Prosperity and Livability*. (The World Bank, 2015).
7. WHO. WHO guideline for the clinical management of exposure to lead. (World Health Organization. Licence: CC BY-NC-SA 3.0 IGO, Geneva, 2021).
8. Kannemadugu, H. B. S., Dorligjav, S., Gharai, B. & M.V.R, S. Satellite-Based Air Pollution Potential Climatology over India. *Water, Air, & Soil Pollution***232**, 365 (2021). <https://doi.org/10.1007/s11270-021-05324-8>
9. Stull, R. B. in *An Introduction to Boundary Layer Meteorology* (ed Roland B. Stull) 1-27 (Springer Netherlands, 1988).
10. Seidel, D. J., Ao, C. O. & Li, K. Estimating climatological planetary boundary layer heights from radiosonde observations: Comparison of methods and uncertainty analysis. *Journal of Geophysical Research: Atmospheres***115** (2010). <https://doi.org/https://doi.org/10.1029/2009JD013680>
11. Kannemadugu, H. B. S. Seasonal Characteristics of Atmospheric Boundary Layer and its Associated Dynamics over Central India. *Asia-Pacific Journal of Atmospheric Sciences* (2019). <https://doi.org/10.1007/s13143-019-00138-5>
12. Xie, F., Wu, D. L., Ao, C. O., Mannucci, A. J. & Kursinski, E. R. Advances and limitations of atmospheric boundary layer observations with GPS occultation over southeast Pacific Ocean. *Atmos. Chem. Phys.***12**, 903-918 (2012). <https://doi.org/10.5194/acp-12-903-2012>

13. Guo, J. *et al.* Investigation of near-global daytime boundary layer height using high-resolution radiosondes: first results and comparison with ERA5, MERRA-2, JRA-55, and NCEP-2 reanalyses. *Atmos. Chem. Phys.***21**, 17079-17097 (2021). <https://doi.org/10.5194/acp-21-17079-2021>
14. Guo, J. *et al.* A merged continental planetary boundary layer height dataset based on high-resolution radiosonde measurements, ERA5 reanalysis, and GLDAS. *Earth Syst. Sci. Data Discuss.***2022**, 1-33 (2022). <https://doi.org/10.5194/essd-2022-150>
15. Hersbach, H. *et al.* The ERA5 global reanalysis. *Quarterly Journal of the Royal Meteorological Society***146**, 1999-2049 (2020). <https://doi.org/10.1002/qj.3803>
16. Holzworth, G. C. Mixing Depths, Wind Speeds and Air Pollution Potential for Selected Locations in the United States. *Journal of Applied Meteorology***6**, 1039-1044 (1967). [https://doi.org/10.1175/1520-0450\(1967\)006<1039:mdwsaa>2.0.co;2](https://doi.org/10.1175/1520-0450(1967)006<1039:mdwsaa>2.0.co;2)
17. Niemeyer, L. E. FORECASTING AIR POLLUTION POTENTIAL. *Monthly Weather Review***88**, 88-96 (1960). [https://doi.org/10.1175/1520-0493\(1960\)088<0088:FAPP>2.0.CO;2](https://doi.org/10.1175/1520-0493(1960)088<0088:FAPP>2.0.CO;2)
18. Goyal, P., Anand, S. & Gera, B. S. Assimilative capacity and pollutant dispersion studies for Gangtok city. *Atmospheric Environment***40**, 1671-1682 (2006). <https://doi.org/10.1016/j.atmosenv.2005.10.057>
19. Lu, C., Deng, Q., Liu, W., Huang, B.-I. & Shi, L.-J. Characteristics of ventilation coefficient and its impact on urban air pollution. *Journal of Central South University***19**, 615-622 (2012).
20. Manju, N., Balakrishnan, R. & Mani, N. Assimilative capacity and pollutant dispersion studies for the industrial zone of Manali. *Atmospheric Environment***36**, 3461-3471 (2002). [https://doi.org/10.1016/S1352-2310\(02\)00306-0](https://doi.org/10.1016/S1352-2310(02)00306-0)
21. Holzworth, G. C. Large-Scale Weather Influences on Community Air Pollution Potential in the United States. *Journal of the Air Pollution Control Association***19**, 248-254 (1969). <https://doi.org/10.1080/00022470.1969.10466483>
22. Miller, M. E. & Niemeyer, L. E. Air Pollution Potential Forecasts—A Year's Experience. *Journal of the Air Pollution Control Association***13**, 205-210 (1963). <https://doi.org/10.1080/00022470.1963.10468166>
23. Nath, S. & Patil, R. S. in *Air Pollution VIII* Vol. 42 (eds C.A. Brebbia, H. Power, & J.W.S Longhurst) Ch. WIT Transactions on Ecology and the Environment, 10 (2000).
24. Goyal, P. & Krishna, T. V. B. P. S. R. Dispersion of pollutants in convective low wind: a case study of Delhi. *Atmospheric Environment***36**, 2071-2079 (2002).
25. Gassmann, M. I. & Mazzeo, N. A. Air Pollution Potential: Regional Study in Argentina. *Environmental Management***25**, 375-382 (2000). <https://doi.org/10.1007/s002679910029>
26. Abiye, O., Akinola, O., Sunmonu, L., Ajao, A. & Ayoola, M. Atmospheric ventilation corridors and coefficients for pollution plume released from an Industrial Facility in Ile-Ife Suburb, Nigeria. *African Journal of Environmental Science and Technology***10**, 338-349 (2016).
27. Sumiya, E. *et al.* Climate Patterns Affecting Cold Season Air Pollution of Ulaanbaatar City, Mongolia. *Climate***11** (2023). <https://doi.org/10.3390/cli11010004>

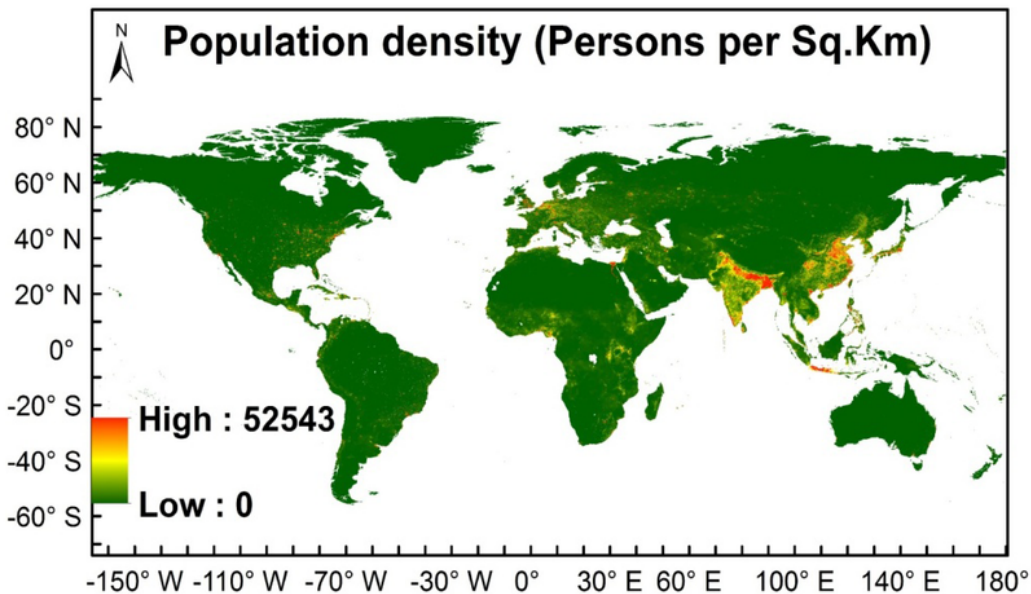
28. Li, X., Jin, L. & Kan, H. Air pollution: a global problem needs local fixes. *Nature***570**, 437-439 (2019).
29. McMichael, A. J. The urban environment and health in a world of increasing globalization: issues for developing countries. *Bulletin of the world Health Organization***78**, 1117-1126 (2000).
30. Duh, J.-D., Shandas, V., Chang, H. & George, L. A. Rates of urbanisation and the resiliency of air and water quality. *Science of the total environment***400**, 238-256 (2008).
31. Gallup, J. L., Sachs, J. D. & Mellinger, A. D. Geography and economic development. *International regional science review***22**, 179-232 (1999).
32. Castells-Quintana, D., Dienesch, E. & Krause, M. Air pollution in an urban world: A global view on density, cities and emissions. *Ecological Economics***189**, 107153 (2021).
[https://doi.org:https://doi.org/10.1016/j.ecolecon.2021.107153](https://doi.org/https://doi.org/10.1016/j.ecolecon.2021.107153)
33. UNDESA, United Nations, Department of Economic and Social Affairs, Population Division. World urbanization prospects: the 2018 revision (2018).
34. Gross, E. *The national air pollution potential forecast program*. Vol. 70 (USAF Environmental Technical Applications Center, 1970).
35. WorldBank. (World Bank, 2019). Sand and Dust Storms in the Middle East and North Africa Region— Sources, Costs, and Solutions. Washington, DC.
36. Xing, Y., Xu, Y., Shi, M. & Lyapustin, A. The impact of PM_{2.5} on the human respiratory system. *Journal of Thoracic Disease***8**, E69-74 (2016).
37. Hammer, M. S. *et al.* Global estimates and long-term trends of fine particulate matter concentrations (1998–2018). *Environmental Science & Technology***54**, 7879-7890 (2020).
38. von Engel, A. & Teixeira, J. A Planetary Boundary Layer Height Climatology Derived from ECMWF Reanalysis Data. *Journal of Climate***26**, 6575-6590 (2013).
[https://doi.org:https://doi.org/10.1175/JCLI-D-12-00385.1](https://doi.org/https://doi.org/10.1175/JCLI-D-12-00385.1)
39. Zhang, Y. *et al.* On the computation of planetary boundary-layer height using the bulk Richardson number method. *Geosci. Model Dev.***7**, 2599-2611 (2014). <https://doi.org:10.5194/gmd-7-2599-2014>
40. Ramon, J., Lledó, L., Torralba, V., Soret, A. & Doblas-Reyes, F. J. What global reanalysis best represents near-surface winds? *Quarterly Journal of the Royal Meteorological Society***145**, 3236-3251 (2019). [https://doi.org:https://doi.org/10.1002/qj.3616](https://doi.org/https://doi.org/10.1002/qj.3616)
41. Vittal Murty, K., Viswanadham, D. & Sadhuram, Y. Mixing heights and ventilation coefficients for urban centres in India. *Boundary-Layer Meteorology***19**, 441-451 (1980).
42. Saha, D., Soni, K., Mohanan, M. & Singh, M. Long-term trend of ventilation coefficient over Delhi and its potential impacts on air quality. *Remote Sensing Applications: Society and Environment***15**, 100234 (2019).
43. Randles, C. *et al.* The MERRA-2 aerosol reanalysis, 1980 onward. Part I: System description and data assimilation evaluation. *Journal of climate***30**, 6823-6850 (2017).
44. Buchard, V. *et al.* The MERRA-2 aerosol reanalysis, 1980 onward. Part II: Evaluation and case studies. *Journal of Climate***30**, 6851-6872 (2017).

45. GMAO, Global Modeling and Assimilation Office (GMAO). *M2TMNXAER–MERRA-2*
tavgM_2d_aer_Nx: 2d, Monthly Mean, Time-Averaged, Single-Level, Assimilation, Aerosol Diagnostics
V5.12.4; Goddard Earth Sciences Data and Information Services Center (GES DISC): Greenbelt, MD,
USA, 2015.

Figures



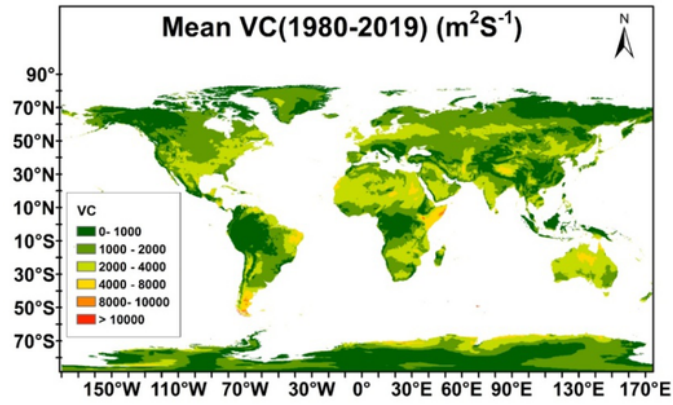
(a)



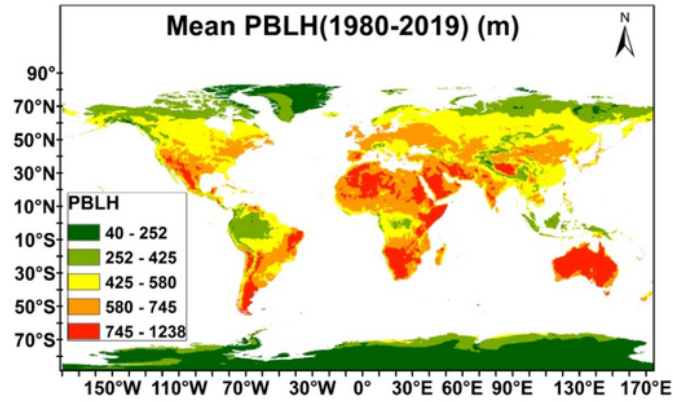
(b)

Figure 1

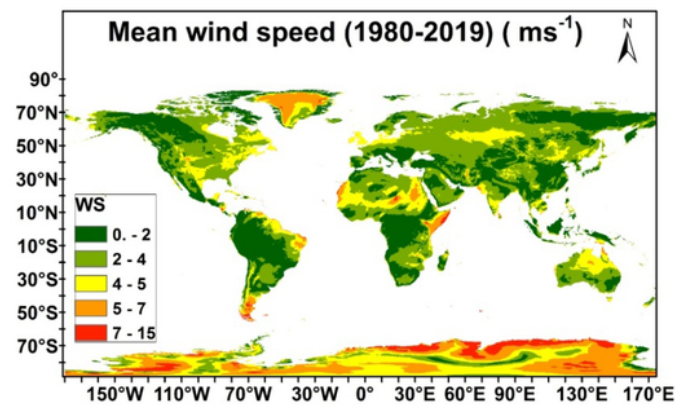
World map showing (a) capital cities of the 30 largest countries in the world and (b) population density



(a)



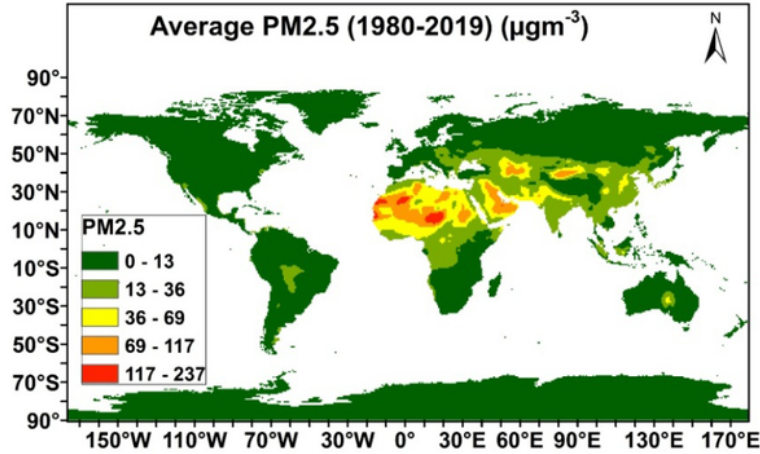
(b)



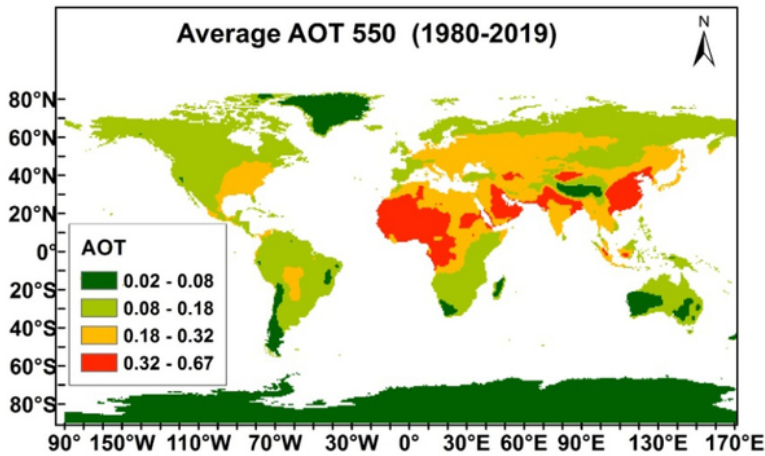
(c)

Figure 2

Spatial variation in annual mean (a) VC/APPI, (b) PBLH, and (c) Wind speed obtained using the monthly data from 40 years (1980-2019)



(a)



(b)

Figure 3

Spatial variations in annual mean(a) PM2.5 and (b) AOT obtained using the monthly data from 40 years (1980-2019)

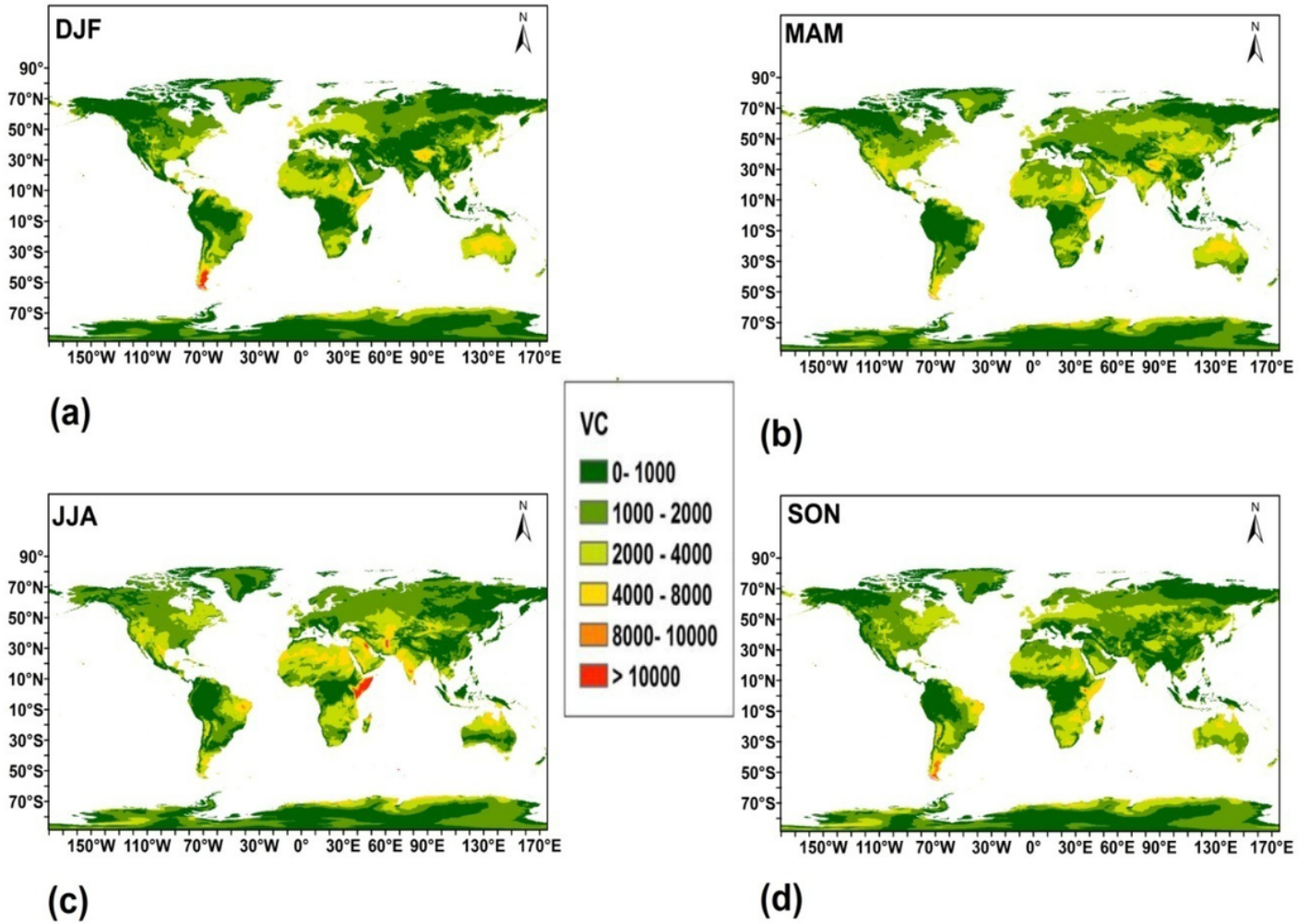
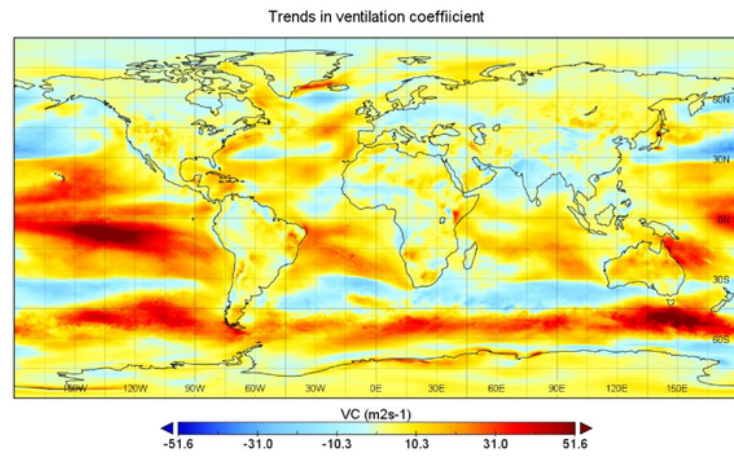
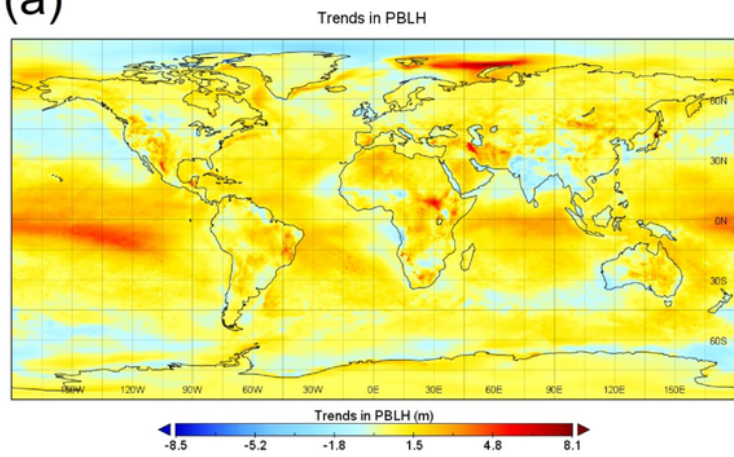


Figure 4

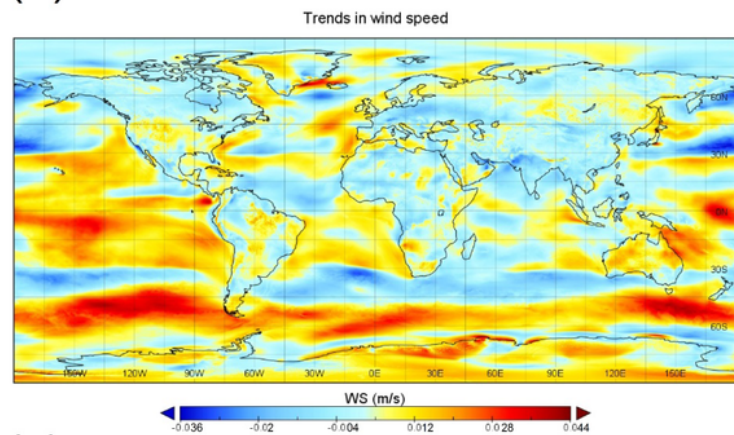
Spatial variation of VC/APPI during different seasons (a) DJF, (b) MAM, (c) JJA, and (d) SON



(a)



(b)

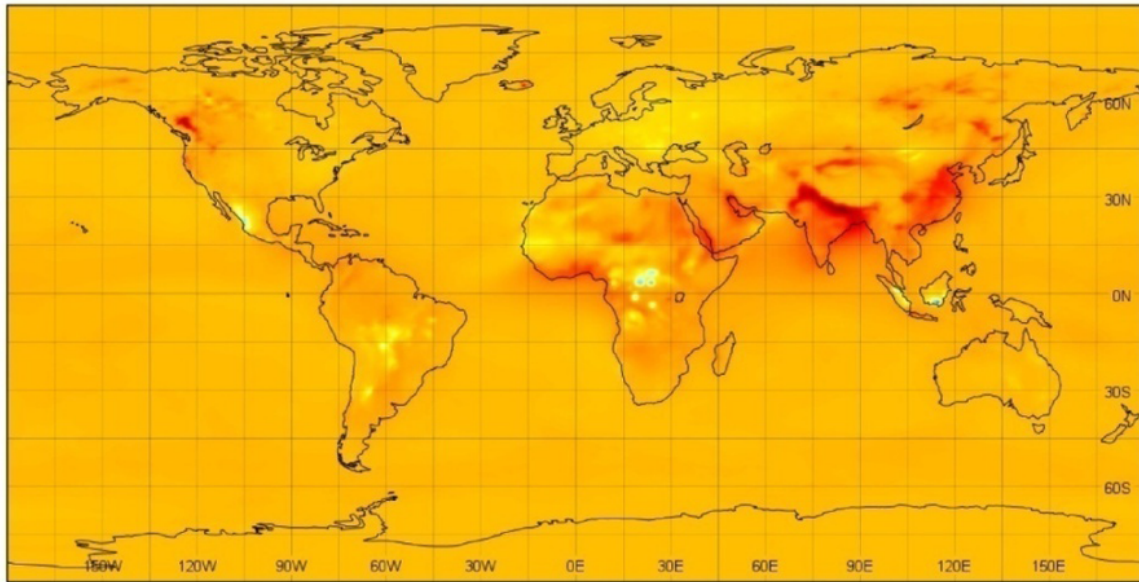


(c)

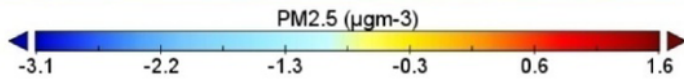
Figure 5

Long term Global annual trends in (a) VC, (b) BLH, and (c) Wind speed

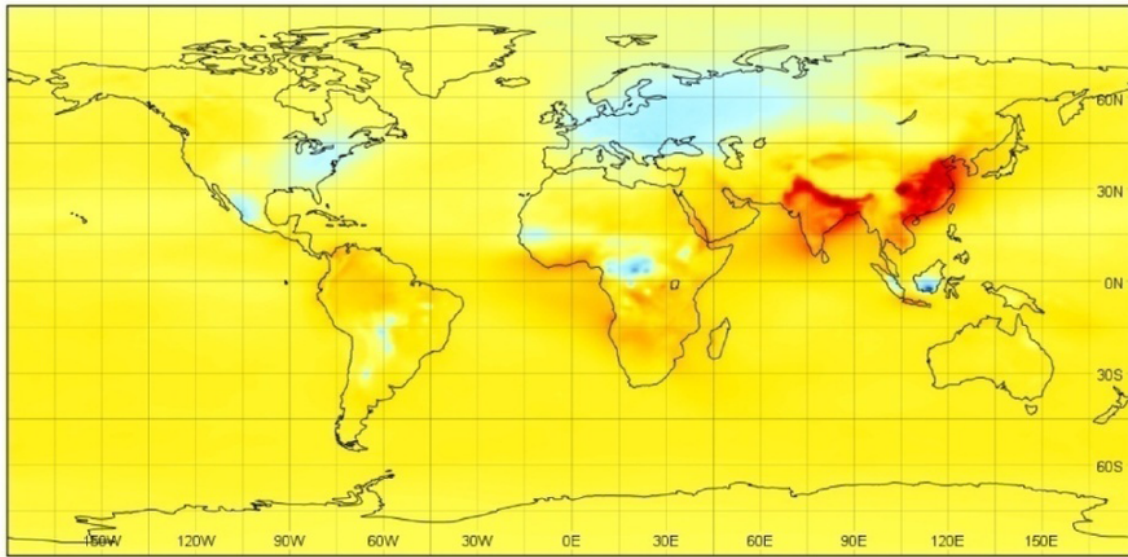
Trends surface PM2.5 concentration



(a)



Trends in Aerosol Optical Thickness (AOT)



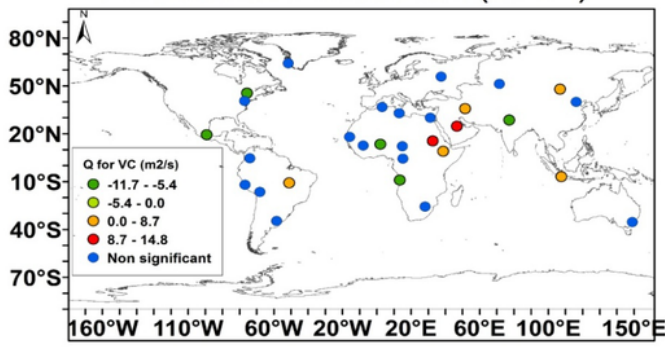
(b)



Figure 6

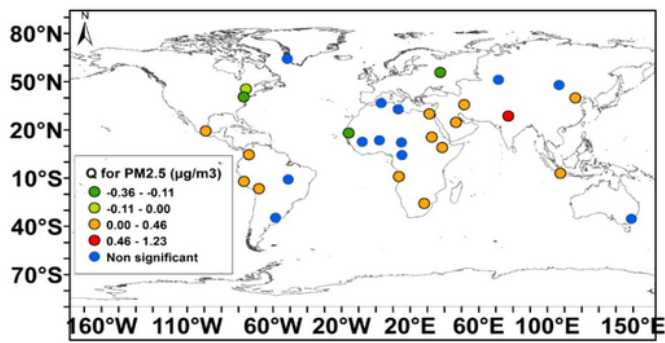
Longterm Global annual trends in (a) PM2.5 and (b) AOT (550nm)

Ventilation coefficient (m^2s^{-1})



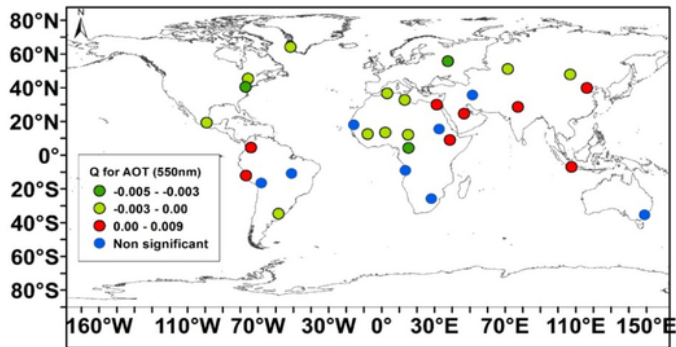
(a)

PM2.5 ($\mu\text{g}\text{m}^{-3}$)



(b)

Aerosol Optical Thickness (AOT)



(c)

Figure 7

Long term annual trends in (a) VC, (b) PM2.5, and (c) AOT (550 nm) over global cities